Seventh International Conference on CFD in the Minerals and Process Industries
CSIRO, Melbourne, Australia
9-11 December 2009

INVESTIGATION OF LIQUID-LIQUID TWO PHASE FLOW IN BIODIESEL PRODUCTION

Karne DE BOER[1*] and Parisa A. BAHRI[1]

[1] School of Engineering and Energy, Murdoch University, Perth Western Australia 6150, AUSTRALIA
*Corresponding author, E-mail address: K.deboer@murdoch.edu.au

ABSTRACT

Over the past two years the Australian biodiesel industry has faced difficult times causing large scale producers to drastically curtail production with some even ceasing operation. This turn of events has highlighted the advantages of small scale production, which are investigated in depth in a companion paper (de Boer and Bahri 2009a). For small scale production to be viable the transesterification reactor at the heart of the process must provide high conversion levels in short time periods. Assessing the performance of a particular reactor design is difficult due to the complex liquid-liquid reaction mixture that is affected by mass transfer, reaction kinetics and component solubility. This paper presents the first step in the development of a CFD model in ANSYS CFX that encapsulates the liquid-liquid flow phenomena observed in the reaction medium. The paper includes an analysis of the reaction mixture focusing on necessary simplifying assumptions, experimental flow visualisation results and an investigation of different simulation settings.

NOMENCLATURE

Variables

D	Diameter (m)
ρ	Density (kg/m^3)
μ	Viscosity (Pa s)
U	Superficial velocity (m/s)
r	Volume fraction

Subscripts

c	Continuous phase
d	Dispersed phase
m	Mixture
p	Pipe

INTRODUCTION

Since the early 1990's biodiesel and other biofuels have rapidly transitioned from backyards and university laboratories into mainstream commercial production. Biodiesel, a fuel derived from vegetable oil or animal fat, is a direct petro-diesel replacement that can significantly reduce emissions including: particulate matter, Carbon Monoxide, Sulphur Dioxide and organics (Sheehan, Camobreco *et al.* 1998). The main driver for the rapid development of this fuel has been increasing pressure on low cost oil supplies and greater public awareness of global warming. Despite the advantages offered by biodiesel, the last two years has seen both the worldwide and Australian biodiesel industry face difficult times

In Australia almost all large scale plants are either producing below their nameplate capacity or have shut down. This turn of events has highlighted the need to consider questions of scale in biodiesel production. Recently, a new production model has been proposed to increase the viability of biodiesel production (de Boer and Bahri 2009a). This concept is built around highly efficient small scale biodiesel plants in the context of regional processing hubs. The focus of this paper is the application of CFD modelling to the reactor at the heart of the biodiesel production process. The CFD model presented in this paper is the first step in the process of developing a complete model for the optimisation of the reactor.

In a typical biodiesel reactor, oil or fat (triglyceride) is converted to Fatty Acid Methyl Esters (FAME) and a co-product glycerol via a catalysed chemical reaction (transesterification). The glycerol is then separated from the FAME with both products subsequently purified. The purified FAME are known as biodiesel while the purified glycerol is sold as a co-product.

It is widely accepted that the conversion of oil to FAME in the reactor proceeds via three consecutive reversible reactions (Noureddini and Zhu 1997):

$$\begin{aligned} &\textbf{Triglyceride + Methanol} \overset{Catalyst}{\Leftrightarrow} \textbf{Diglyceride + FAME} \\ &\textbf{Diglyceride + Methanol} \overset{Catalyst}{\Leftrightarrow} \textbf{Monoglyceride + FAME} \\ &\textbf{Monoglyceride + Methanol} \overset{Catalyst}{\Leftrightarrow} \textbf{Glycerol + FAME} \end{aligned} \quad (1)$$

The reactant intermediates (diglycerides and monoglycerides) appear in small concentrations during the reaction and are considered contaminants in the final product. Different catalysts have been investigated in this reaction including homogeneous (liquid) (Vicente, Martinez *et al.* 2003), heterogeneous (solid) (Lotero, Goodwin *et al.* 2006), enzymes(Akoh, Chang *et al.* 2007) and even no catalyst at extreme conditions (Pinnarat and Savage 2008). Despite this wide variety, almost all commercial plants throughout the world currently use an alkaline homogeneous catalyst (Sodium or Potassium Methylate) (Mittelbach and Remschmidt 2006). At this stage homogeneous catalyst reactions are the most feasible for small scale production with only a handful of commercial solid catalyst and enzymatic processes.

The step-wise reaction, collectively called the transesterification or methanolysis reaction is commonly shown in the form given in Equation 2.

$$\textit{Oil + 3Methanol} \rightarrow \textit{Glycerol + 3FAME} \quad (2)$$

REACTION MEDIUM

Investigations into the transesterification reaction have shown that it transitions from a multiphase (liquid-liquid)

mixture (oil and methanol) to another biphasic mixture (FAME and glycerol) via a pseudo-single phase emulsion (Noureddini and Zhu 1997; Stamenkovic, Lazic *et al.* 2007; Stamenkovic, Todorovic *et al.* 2008). Throughout the reaction a continuous non-polar phase (Oil, FAME reaction intermediates) and a dispersed polar phase (methanol, glycerol and catalyst) are present with the composition of the phases constantly changing. Due to the nature of the reaction medium the rate of reaction is affected by chemical kinetics, mass transfer and component solubility.

The kinetic rate constants for the three stepwise reactions shown in Equation 1 have been determined by a number of authors (Darnoko and Cheryan 2000; Freedman, Butterfield *et al.* 1986; Karmee, Chandna *et al.* 2006; Noureddini and Zhu 1997; Vicente, Martinez *et al.* 2005b). These studies do not explicitly account for the heterogeneous nature of the reaction, consequently, mass transfer and solubility effects are incorporated into the rate constants (Doell, Konar *et al.* 2008). Despite this common simplification the reaction progression has been shown to be sigmoidal and can be characterised by three stages as shown in Figure 1. The first stage is characterised by an initial slow rate of reaction; the second by a rapid progression up to approximately 80% conversion and finally a third stage as equilibrium is approached (Noureddini and Zhu 1997).

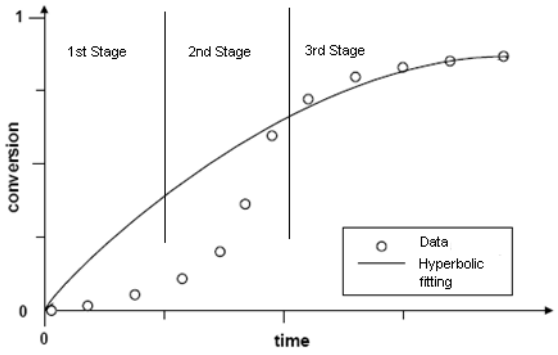

Figure 1: Sigmoidal reaction progression

In the first stage the concentration of oil in the methanol droplets (where the majority of the catalyst resides) is low, requiring significant agitation to reach saturation levels (Boocock, Konar *et al.* 1996). In this stage it is most likely that the rate of mass transfer between the phases is slower then the chemical rate, thus in this stage, mass transfer is the controlling factor (Noureddini and Zhu 1997; Stamenkovic, Lazic *et al.* 2007)

In the second stage, the reaction rate rapidly increases. Stamekovic *et al.,* (2007; 2008) observed that this increase coincided with a reduction in droplet size. As the droplet size decreases, the area of the polar phase and thus the mass transfer rate increases, explaining the sudden jump in reaction rate. The reaction medium during this stage has been described by some as a pseudo single phase emulsion (Ma, Clements *et al.* 1999; Zhou and Boocock 2006) . Different authors have attributed the self enhanced mass transfer rate to the surfactant action of the reaction intermediates (Boocock, Konar *et al.* 1998; Stamenkovic, Lazic *et al.* 2007), while others have attributed it to the solvent properties of FAME (Noureddini and Zhu 1997).

In the third step, the reaction rate rapidly curtails as equilibrium is approached. It is proposed that this sudden drop is due to the breaking of the single phase emulsion as glycerol is formed, resulting in the catalyst preferentially dissolving in the polar phase. With almost all of the un-reacted glycerides residing in the non-polar phase this results in a very slow approach to equilibrium. It is therefore proposed that in the final stage, it is the solubility of components and not the rate of mass transfer which limits the reaction rate. This was also observed in the reverse reaction (glycerolysis of FAME) by Kimmel (2004) and Negi (2006).

In most industrial operations the methanolysis reaction is conducted between 50 and 70°C with significant mixing. Under these conditions it is reasonable to assume that the effect of mass transfer limitations in the first stage is negligible (Noureddini and Zhu 1997; Vicente, Martinez *et al.* 2005a). In the second stage, the absence of mass transfer limitations allows the reaction to be treated as a single phase. Consequently, both the first and second stages of the reaction can be adequately described by second order kinetics models available in the literature that ignore the multiphase behaviour of the reaction.

This second order model could be extended to the third reaction step, however, the high difference in density can result in the glycerol laden polar phase separating from the non-polar phase causing the reaction to cease prematurely. This is especially true for tubular reactors in which the flow can stratify on long straight runs with insufficient turbulence.

CFD modelling was identified as an excellent tool to investigate the flow behaviour of the two phases in tubular reactors during the final stage of the reaction. The development of such a CFD model allows different reactor designs (diameter and length) and operating conditions (flow-rate) to be easily trialled. The remainder of this paper firstly introduces the experimental work conducted on a tubular reactor and secondly discusses the first phase of CFD model development in the development of an overall model for optimisation.

EXPERIMENTAL RESULTS

To provide qualitative direction and validation for the CFD model a novel high temperature and pressure tubular reactor developed by Bluediesel PTY LTD was used to conduct flow visualisation studies. The reactor consists of multiple straight runs (5.8m) followed by tight (180°) bends. Before the tubular reactor a mixing tank is present in which the first two stages of the reaction rapidly occur. As a result, the reactants typically enter the tubular reactor 80% reacted and thus in the final stage of the reaction.

To allow visualisation of the fluid flow, a 4m run of thick walled borosilicate glass tube was plumbed into the midpoint of the reactor via 2 isolating valves. This tube had an internal diameter of 11mm (required to achieve a pressure rating in excess of 300psi). Refined Bleached Dried (RBD) Coconut oil (Procter and Gamble, Australia) was the feedstock which had been reacted for a long

period of time at typical conditions to drive the reaction to completion. Food colouring (green, 50ml) was added to the mixing tank before the reactor to provide a clear distinction between the polar and non-polar phase. The food colouring preferentially dissolves in the polar phase and provides a simple but effective method for multiphase flow visualisation (Zhou and Boocock 2006).

The flow-rate was controlled using a variable speed drive on the high pressure pump that drove the reaction medium through the reactor. The flow visualisations for representative conditions are summarised in Figure 2. The superficial flow velocities for each case were calculated using the volumetric flow-rate and pipe diameter. A full video of results is provided as an attachment to this paper. This video clearly shows the transition from stratified to fully dispersed flow as the flow-rate is increased.

Apart from the tube diameter and flow velocity, the key variables that determine flow behaviour are the viscosity and density of the two phases. A sample was taken of the reaction medium and allowed to settle. The viscosity and density of each phase were measured up to 65° and extrapolated to the reaction midpoint temperature (~91°C) according to the method in de Boer *et al.*, (2009b) and are shown in Table 1.

Table 1: Fluid Properties

Phase	**Density (kg/m^3)**	**Viscosity (cP)**
Polar	982.3	2.335
Non-polar	819	1.109

DISCUSSION

The flow visualisation results in Figure 2 show that the two phase flow regime varies significantly with flow velocity. At low velocities, the flow stratifies, at higher velocities the polar phase becomes dispersed in the continuous non-polar phase. The first is undesirable as it limits mass transfer, while the second represents the intended design with each phase having access to the other and component solubility being the only limitation. When considering various tubular reactor designs (diameter and length) and operating conditions (flow-rate) it is necessary to predict the flow regime to prevent stratification.

In single phase flow, the dimensionless Reynolds number (Re), shown in Equation 3, is used to predict the onset of turbulent flow.

$$\mathrm{Re}_{2\,\mathrm{Phase}} = \frac{\rho_{\mathrm{m}} D_p U}{\mu_m} \qquad (3)$$

To account for two phase flow, the volume averaged densities and viscosities were used as shown in Equations 4 and 5. The results of these calculations are provided in Table 2 which contains the Re for the three different superficial flow velocities shown in Figure 2.

$$\rho_{\mathrm{m}} = r_c \rho_c + r_d \rho_d \qquad (4)$$

$$\mu_m = r_c \mu_c + r_d \mu_d \qquad (5)$$

Spriggs (1973) and many other authors suggest that true laminar flow exists below Re of 2000, with a transition from laminar to turbulent flow between Reynolds numbers of 2000 and 3000. This criterion provides a reasonable match with the transition to turbulent flow, indicated by the dispersion of the polar phase, recorded in Figure 2.

Table 2: Reynolds Number

Superficial Velocity	**Reynolds Number**
0.16 m/s (Figure 2a)	1148
0.28 m/s (Figure 2b)	2009
0.41 m/s (Figure 2c)	2942

Although the application of Reynolds Number provides a reasonable initial design estimate of the flow regime, it masks the behaviour of the flow throughout the reactor especially around bends and in turbulator elements. The application of CFD modelling to this particular problem will provide further insight into the effect of reactor design on flow regime. The difficulty in applying CFD modelling to this particular problem centres on the complexity involved in predicting the transition between stratified and non-stratified (dispersed flow). That is, the CFD model must be either set up as a stratified flow problem (Vallée, Höhne *et al.* 2008) or it must be setup as a dispersed flow problem (Walvekar, Choong *et al.* 2009).

Although there is no known research into CFD models for two phase liquid-liquid flow in biodiesel production, there has been extensive work conducted into two phase flows of oil and water. In biodiesel production the polar phase is more dense and viscous than the non-polar phase.

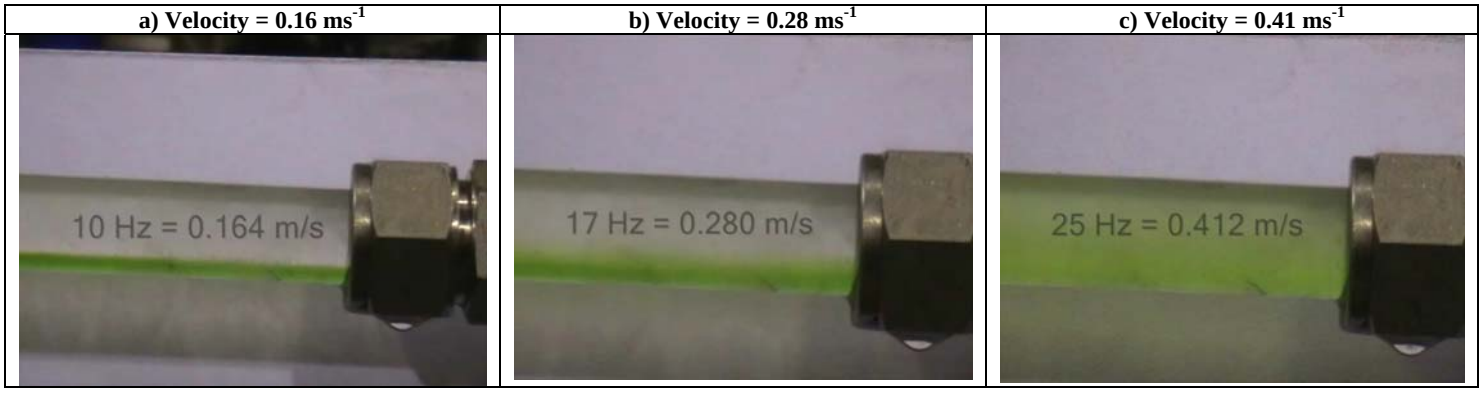

Figure 2: Summary of Flow Visualisation Results

While in the oil and gas industry the oil is typically less dense and more viscous then the water phase (Hussain 2004). Despite these differences, it is extremely worthwhile to examine these large bodies of knowledge before developing the CFD model in this novel field.

The work of Al-Wahaibi *et al.,*(2007; 2009a; 2009b; 2007) provides significant insight into the transition between horizontal stratified and dispersed flow. The fundamental hypothesis of these works can be summarised in the quote below:
"When the flow rates of oil and water increase, interfacial waves appear which are initially long compared to the pipe diameter. These waves will grow until they reach a certain wavelength and amplitude at which point the crests will break and drops start forming." (Al-Wahaibi and Angeli 2007)

The experimental results contained in the attached video clearly show the onset of these waves as the flow-rate is gradually increased. The instability generated by these waves continues to grow with increasing flow velocity until the polar phase is completely entrained in the non polar phase.

In investigations using air and water for Nuclear reactor design Vallee *et al.,* (2008) developed a transient 2 phase model in CFX that effectively modelled waves at the water/air interface. Walvekar *et al.,* (2009), on the other hand used Fluent 6.2 to develop a model of dispersed oil-water turbulent flow in a horizontal tube.

It is thus suggested that liquid-liquid biodiesel flow in tubular reactors requires two separate models, that is, one model that captures the stratified flow phenomena and another model that captures the dispersed flow phenomena. Furthermore, the Re could be used as the criterion to determine which model should be applied. In the remainder of this paper the focus is on the dispersed model as this is the intended operating mode of the reactor.

MODEL DEVELOPMENT

ANSYS CFX 12 provides functionality to model dispersed two phase flow in 3 dimensions, i.e., immiscible liquid droplets in other liquids, via two different methods: Eulerian-Eulerian and Lagrangian particle tracking method. The former was chosen in this case because the polar phase volume fraction remains virtually constant at 15% in the final stage of the reaction. This experimental work as well as recent papers from Stamenkovic (2007; 2008) clearly show that the polar phase is dispersed in the non-polar phase at this volume fraction.

The dimensions of the tube were that of the experimental setup (Diameter of 11mm and length of 4m). A three dimensional mesh for the tube was developed using the ANSYS meshing tool in Workbench 12. A mesh refinement study was performed to determine the optimal mesh arrangement which is shown in Figure 3. This is a swept mesh (200 divisions) with inflation, edge controls and size controls resulting in 399,800 elements.

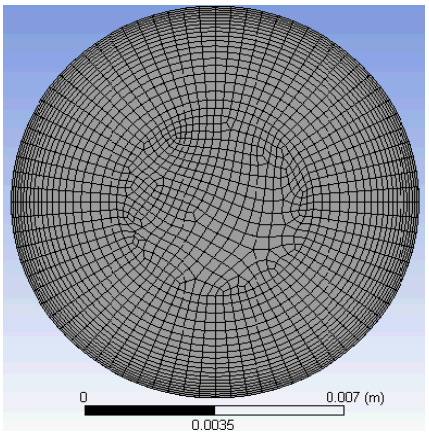

Figure 3: Refined Mesh

To reduce computational time, tubes are typically split in half and a symmetry plane is inserted, however, comparisons between half and full tube showed a difference of up to 5% in the bottom and top phase fractions. It was consequently decided to keep the full tube to reduce unnecessary error.

The key variables used to define the simulation are shown in Table 3.

Table 3: Simulation Settings

Variable/Setting	Typical Value
Dispersed droplet diameter	0.055mm
Free surface model	None
Homogeneity	Non homogeneous
Turbulence (Fluid dependant)	*Continuous:* k-Epsilon *Dispersed:* Dispersed phase zero equation
Surface tension coefficient	0.0292 J/m^2
Drag Force	Ishii-Zuber

The droplet diameter was taken from the work of Stamenkovic *et al.,* (2007; 2008) in which experimental measurement showed a constant value between 0.05 and 0.06mm in the final stage of the reaction. The surface tension coefficient was required for the Ishii-Zuber correlation and was taken from (Allen, Watts *et al.* 1999).

The boundary conditions for this model are summarised in Table 4. For the studies performed here, the inlet turbulence intensity was set at 5% which is typical for pipe flows (Abraham, Sparrow *et al.* 2008).

Table 4: Boundary Conditions

Boundary	Value
Inlet (Normal speed)	0.41ms^{-1}
Outlet (Average Static Pressure)	20psi
Tube wall	Smooth, no-slip wall

Two fluids were defined (polar phase and non-polar phase) with the properties listed in Table 1. Buoyancy was activated, as this is the driving force for phase separation in this model. Besides the buoyancy force the main force (ignoring turbulence induced viscous stresses) acting on the particles is the drag force. Parametric studies conducted with the other particle forces (lift, virtual mass and wall lubrication) indicated that these have a negligible

effect on the polar phase hold-up, which is in agreement with the work of Hussain (2004).

In the sparsely distributed particle regime, the Ishii-Zuber drag coefficient is dependent on the Eotovos number which is calculated using the surface tension. It was noticed that the surface tension had no effect on the flow regime. Further investigation revealed that the drag coefficient was being determined using dense particle effects which are based on the particle Reynolds number no the Eotovos number (ANSYS 2009).

SIMULATION RESULTS AND DISCUSSION

The simulation defined by the settings in Table 3 and Table 4 reached convergence in less than 3 hrs on 4 cores of a dual, quad core cpu (3Ghz Xeon) server. Convergence was defined by RMS residuals less than 10^{-4} and imbalances (conservation) less than 10^{-2} for all variables. Simulations of the other two velocities (0.28m/s and 0.16 m/s), however, failed to converge reinforcing the idea that the dispersed model is inappropriate for these lower velocity conditions. Polar phase volume fractions for the cross-sections at the midway and end point of the tube are shown in Figure 4 and Figure 5 respectively.

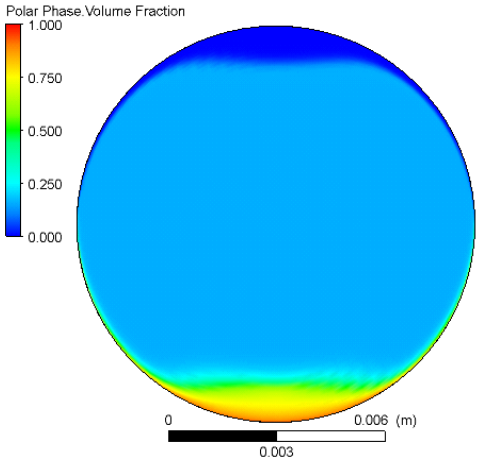

Figure 4: Midway (2m) polar phase distribution

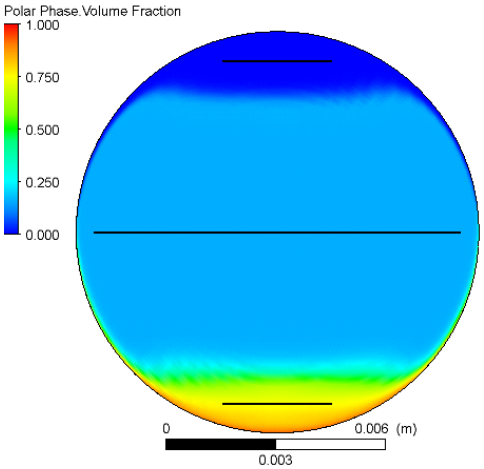

Figure 5: Outlet (4m) polar phase volume fraction

Table 5 provides the average polar phase volume fraction at the locations (black lines) shown in Figure 5. These combined results show the flow slowly stratifying over the length of the pipe which is contrary to the experimental results shown in Figure 2. This was also observed in the work of Hussain (2004) in which the simulated oil and water flow stratified, while experimental results showed mixing.

Table 5: Polar phase volume fractions

Location	Average Polar Phase Volume Fraction
Bottom	0.74
Middle	0.15
Top	0.00

To overcome this mismatch between model and reality another droplet force or instability is required. The current work is focused on achieving convergence in simulations incorporating the turbulent dispersion force. If these simulations provide a better reflection of reality, the next steps are to incorporate reaction kinetics and component solubility while trailing more complex geometries.

CONCLUSION

This paper provides the first step in the development of a CFD model to encapsulate liquid-liquid flow in a biodiesel transesterification reactor. Ultimately this model will provide a method for optimisation of the biodiesel reactor for small scale production in regional processing hubs. Further work is focused on incorporating the turbulent dispersion force so that the simulation matches the experimental results

The next phase of model development will involve incorporating component solubility and reaction kinetics into the CFD model while also trialling more complex geometries. The final phase of model development is the construction of a CFD model for the stratified flow regime It is also necessary that further experimental work is conducted to quantitatively verify the CFD results of this and future models.

REFERENCES

ABRAHAM J.P., SPARROW E.M., TONG J.C.K. (2008) Breakdown of Laminar Pipe Flow into Transitional Intermittency and Subsequent Attainment of Fully Developed Intermittent or Turbulent Flow. *Numerical Heat Transfer, Part B: Fundamentals: An International Journal of Computation and Methodology* **54**, 103-115.

AKOH C.C., CHANG S.-W., LEE G.-C., SHAW J.-F. (2007) Enzymatic Approach to Biodiesel Production. *Journal of Agricultural and Food Chemistry* **55**, 8995-9005.

AL-WAHAIBI T., ANGELI P. (2007) Transition between stratified and non-stratified horizontal oil-water flows. Part I: Stability analysis. *Chemical Engineering Science* **62**, 2915-2928.

AL-WAHAIBI T., ANGELI P. (2009a) Onset of entrainment and degree of dispersion in dual continuous horizontal oil-water flows. *Experimental Thermal and Fluid Science* **33**, 774-781.

AL-WAHAIBI T., ANGELI P. (2009b) Predictive model of the entrained fraction in horizontal oil-water flows. *Chemical Engineering Science* **64**, 2817-2825.

AL-WAHAIBI T., SMITH M., ANGELI P. (2007) Transition between stratified and non-stratified horizontal oil-water flows. Part II: Mechanism of drop formation. *Chemical Engineering Science* **62**, 2929-2940.

ALLEN C.A.W., WATTS K.C., ACKMAN R.G., PEGG M.J. (1999) Predicting the viscosity of biodiesel fuels from their fatty acid ester composition. *Fuel* **78**, 1319-1326.

ANSYS (2009) 'ANSYS CFX-Solver Modeling Guide.' Available from: ANSYS.

BOOCOCK D.G.B., KONAR S.K., MAO V., LEE C., BULIGAN S. (1998) Fast formation of high-purity methyl esters from vegetable oils. *J. Am. Oil Chem. Soc.* **75**, 1167-1172.

BOOCOCK D.G.B., KONAR S.K., MAO V., SIDI H. (1996) Fast one phase oil-rich process for the preparation of vegetable oil methyl esters. *Biomass and Bioenergy* **11**, 43-50.

DARNOKO D., CHERYAN M. (2000) Kinetics of palm oil transesterification in a batch reactor. *JAOCS* **77**, 1263-1267.

DE BOER K., BAHRI P.A. (2009a) Forging Ahead with Small Scale Production: A different Approach for the Australian Biodiesel Industry in Difficult Times. *In Press*.

DE BOER K., BAHRI P.A. (2009b) Viscosity and Density of the phases in the biodiesel reaciton medium. *In Press*.

DOELL R., KONAR S.K., BOOCOCK D.G.B. (2008) Kinetic parameters of homogeneous transmethylation of soybean oil. *J. Am. Oil Chem. Soc.* **85**, 271-276.

FREEDMAN B., BUTTERFIELD R.O., PRYDE E.H. (1986) Transesterification kinetics of soybean oil. *JAOCS* **63**, 1375-1380.

HUSSAIN S.A. (2004) Experimental and Computational Studies of Liquid-Liquid Dispersed Flows. Univeristy of London.

KARMEE S.K., CHANDNA D., RAVI R., CHADHA A. (2006) Kinetics of base catalyzed transesterification of triglycerides from pongamia oil. *J. Am. Oil Chem. Soc.* **83**, 873-877.

KIMMEL T. (2004) Kinetic Investigation of the base-catalysed glycerolysis of Fatty Acid Methyl Esters Technical University of Berlin.

LOTERO E., GOODWIN J.G., BRUCE D.A., SUWANNAKARN K., LIU Y., LOPEZ D.E. (2006) The catalysis of Biodiesel synthesis. *Catalysis* **19**, 41-83.

MA F., CLEMENTS D., HANNA M. (1999) The effect of mixing on transesterification of beef tallow. *Bioresource Technology* **69**, 289-293.

MITTELBACH M., REMSCHMIDT C. (2006) 'Biodiesel the comprehensive handbook.' (Martin Mittelbach: Vienna)

NEGI D.S. (2006) Base Catalyzed Glycerolysis of Fatty Acid Methyl Esters: Investigations Toward the Development of a Continuous Process. Technical University of Berlin.

NOUREDDINI H., ZHU D. (1997) Kinetics of Transesterification of soybean oil. *Journal of the American Oil Chemists' society* **74**, 1457-1463.

PINNARAT T., SAVAGE P.E. (2008) Assessment of noncatalytic biodiesel synthesis using supercritical reaction conditions. *Industrial & Engineering Chemistry Research* **47**, 6801-6808.

SHEEHAN J., CAMOBRECO V., DUFFIELD J., GRABOSKI M., SHAPOURI H. (1998) 'Life Cycle inventory of biodiesel and petroleum diesel for use in an urban bus.' National Renewable energy Laboratory, NREL/SR-580-24089. Available from: http://www.nrel.gov/docs/legosti/fy98/24089.pdf.

SPRIGGS H.D. (1973) Comments on Transition from Laminar to Turbulent Flow. *Industrial & Engineering Chemistry Fundamentals* **12**, 286-290.

STAMENKOVIC O.S., LAZIC M.L., TODOROVIC Z.B., VELJKOVIC V.B., SKALA D.U. (2007) The effect of agitation intensity on alkali-catalyzed methanolysis of sunflower oil. *Bioresource Technology* **98**, 2688-2699.

STAMENKOVIC O.S., TODOROVIC Z.B., LAZIC M.L., VELJKOVIC V.B., SKALA D.U. (2008) Kinetics of sunflower oil methanolysis at low temperatures. *Bioresource Technology* **99**, 1131-1140.

VALLÉE C., HÖHNE T., PRASSER H.-M., SÜHNEL T. (2008) Experimental investigation and CFD simulation of horizontal stratified two-phase flow phenomena. *Nuclear Engineering and Design* **238**, 637-646.

VICENTE G., MARTINEZ M., ARACIL J. (2003) Integrated Biodiesel production: A comparison of different homogeneous catalyst systems. *Bioresource Technology*, 297-305.

VICENTE G., MARTINEZ M., ARACIL J. (2005a) Optimization of Brassica carinata oil methanolysis for biodiesel production. *J. Am. Oil Chem. Soc.* **82**, 899-904.

VICENTE G., MARTINEZ M., ARACIL J., ESTEBAN A. (2005b) Kinetics of Sunflower Oil Methanolysis. *Ind. Eng. Chem. Res.* **44**, 5447-5454.

WALVEKAR R.G., CHOONG T.S.Y., HUSSAIN S.A., KHALID M., CHUAH T.G. (2009) Numerical study of dispersed oil-water turbulent flow in horizontal tube. *Journal of Petroleum Science and Engineering* **65**, 123-128.

ZHOU W., BOOCOCK D.G.B. (2006) Phase behavior of the base catalyzed transesterification of soybean oil. *J. Am. Oil Chem. Soc.* **83**, 1041-1045.

